JCTC Journal of Chemical Theory and Computation

Increasing the Efficiency of Free Energy Calculations Using Parallel Tempering and Histogram Reweighting

Steven W. Rick*

Department of Chemistry, University of New Orleans, New Orleans, Louisiana 70148, and Chemistry Department, Southern University of New Orleans, New Orleans, Louisiana 70126

Received August 19, 2005

Abstract: Free energy calculations from molecular simulations using thermodynamic integration or free energy perturbation require long simulation times to achieve sufficient precision. If entropic and enthalpic components of the free energy are desired, then the computational requirements are larger still. Here we present how parallel tempering (PT) Monte Carlo and weighted histogram analysis method (WHAM) can be used to improve the efficiency of free energy calculations. For both methods, which can be used separately or together, simulations at more than one temperature are performed. The same additional temperatures are often used to determine entropy changes. The results, for the aqueous solvation of *n*-butane and methane, show noticeable improvement in the precision of the free energy and entropy changes. The PT and WHAM methods can give similar error bars as conventional molecular dynamics in half the simulation time. The methods offer an efficient procedure for calculating free energy, entropy, and enthalpy changes in which free energy calculations are performed in parallel for a small number of closely spaced temperatures (for example, as here, at three temperatures: 298 K and 298 ± 15 K), and WHAM is used to enhance the data at each temperature.

I. Introduction

Free energy differences for processes involving changes in noncovalent interactions can be calculated through free energy perturbation (FEP) or thermodynamic integration (TI).[1,2] These methods give an exact free energy change, ΔG, and are limited only by the accuracy of the potential models and large computational requirements. The calculation of fully converged ΔG values can involve extensive sampling of phase space as demonstrated by one recent study which used over 300 ns of simulation time to calculate a single ΔG value.[3] More thermodynamic information can be found by calculating ΔG over a range of temperatures, from which changes in entropy, enthalpy, and heat capacity can be found.[4−10] The calculations at different temperatures are from independent simulations. By combining the simulations at different temperatures, the efficiency of the free energy calculations may be improved in two ways. First, the sampling over phase space at one temperature can be enhanced from phase space sampling at different temperatures using parallel tempering (PT).[11−14] Second, the data from one temperature can used to determine ensemble averages at another temperature using WHAM.[15,16]

The most common free energy methods are the potential of mean force (PMF), in which free energies as a function of a physical coordinate is determined, and FEP and TI, in which a free energy for adding particles to a system is determined. In these methods, the potential energy of the system, $E(\boldsymbol{r})$, is scaled by a parameter λ which can couple to a biasing potential for PMF or the interaction of the added particles in TI or FEP, as

$$E(\boldsymbol{r}) = E_0(\boldsymbol{r}) + \lambda V(\boldsymbol{r}) \tag{1}$$

A variety of methods use replica exchange and WHAM in combination with PMF, FEP, and TI (see Table 1). Parallel tempering can improve sampling efficiency by running several identical replicas of the system at different temperatures. In replica exchange, the replicas are simulated not

* Corresponding author e-mail: srick@uno.edu.

10.1021/ct050207o CCC: $33.50
Published on Web 05/27/2006

Table 1. Free Energy Methods, Free Energy Perturbation (FEP), Potential of Mean Force (PMF), and Thermodynamic Integration (TI), Which Use the Weighted Histogram Analysis Method (WHAM) and Replica Exchange Swaps in Both Temperature, T, and Hamiltonian, λ, Variables

free energy method	swaps	WHAM	ref
PMF		λ, T	16
FEP		λ	17
TI,FEP	λ or T		18
PMF	λ, T	λ, T	19
TI	T	T	present work

only at different temperatures but also other thermodynamic conditions or Hamiltonians.[13,14] Each replica is simulated with conventional Monte Carlo (MC) or molecular dynamics (MD), and, in addition to the local sampling of phase space, global moves are attempted which involve exchanges between replicas at, for example, different temperatures or values of λ. Swaps in either T and λ (but not both) were used by Woods, Essex, and King in combination with FEP and TI,[18] and swaps in both T and λ were used by Sugita, Kitao, and Okamoto with PMF.[19] Reference 19 also described a a FEP method using replica exchange and WHAM, but this method was not applied. Histogram reweighting provides a method to reweight data generated with a different Hamiltonian or temperature for the desired Hamiltonian or temperature. The use of WHAM is extremely common for PMF calculations, and, due to the similarities in the energies given by eq 1, what might be termed FEP or PMF is somewhat arbitrary in certain cases. One method combining FEP and WHAM was described by Nina, Beglov, and Roux.[17] Histogram reweighting can be used to find a system's free energy as a function of temperature.[15,20−24] The method of expanded ensembles provides another method for finding free energy as a function of temperature.[25] Some of the WHAM studies have used parallel tempering to aid in the simulations at different temperatures.[20,22−24]

This paper examines how PT and WHAM can improve the convergence of the ensemble average quantities that are needed by TI to find ΔG and entropy changes. Calculations are done for the hydration free energy of methane and of butane. For methane, a united atom, single interaction site model is used, so this calculation is predominantly dependent on the solvent degrees-of-freedom. For butane, which has important intramolecular degrees-of-freedom, the calculation is dependent on both solute and solvent coordinates.

II. Methods

Thermodynamic Integration. The free energy difference between two systems can be obtained by thermodynamic integration from

$$\Delta G = \int_0^1 \left\langle \frac{\mathrm{d}E_\lambda}{\mathrm{d}\lambda} \right\rangle_\lambda \mathrm{d}\lambda \tag{2}$$

where λ is a parameter that connects the two systems, E_λ is the λ dependent Hamiltonian, and $\langle \cdots \rangle_\lambda$ corresponds to an isothermal, isobaric ensemble average with potential energy, E_λ. In the examples studied here, the $\lambda = 0$ state corresponds to pure water, and $\lambda = 1$ corresponds to water with the addition of a single solute molecule, butane or methane. The entropy change, ΔS, can be found by taking the temperature derivative of eq 2 giving[26−30]

$$\Delta S = \frac{-1}{kT^2} \int_0^1 \left(\left\langle (PV + E_\lambda) \frac{\partial E_\lambda}{\partial \lambda} \right\rangle_\lambda - \langle PV + E_\lambda \rangle_\lambda \left\langle \frac{\partial E_\lambda}{\partial \lambda} \right\rangle_\lambda \right) \mathrm{d}\lambda \tag{3}$$

Heat capacity changes can be found from the second temperature derivative of eq 2.[9] Interactions between the solvent and the solute are scaled by the parameter λ using the separation-shifted scaling method of Zacharias et al., which eliminate the singularities in the potential energy terms as λ approaches zero.[31] The λ dependent energy is

$$E_\lambda = E_{\mathrm{water,water}} + \lambda \sum_i \sum_j 4\epsilon_{ij} \left[\left(\frac{\sigma_{ij}^2}{r_{ij}^2 + \delta(1-\lambda)} \right)^6 - \left(\frac{\sigma_{ij}^2}{r_{ij}^2 + \delta(1-\lambda)} \right)^3 \right] + q_i q_j / (r_{ij}^2 + \delta(1-\lambda))^{1/2} \tag{4}$$

where the sum over i is for solvent atoms and over j is for solute atoms, ϵ_{ij} and σ_{ij} are the Lennard-Jones parameters, q_i is the charge of atom i, r_{ij} is the distance between i and j, and δ is the shifting parameter that avoids the singularities at $r_{ij} = 0$. The value of δ is chosen so that the integrand is as linear as possible, giving the most direct path from $\lambda = 0$ to $\lambda = 1$.[31,32] In this study, δ is set equal to 7 Å^2. The entropy change can also be found using a finite difference expression for the temperature derivative

$$\Delta S = -[\Delta G(T + \Delta T) - \Delta G(T - \Delta T)]/2\Delta T \tag{5}$$

This requires calculating ΔG at two additional temperatures ($T \pm \Delta T$). The finite difference expression is strictly valid only for small ΔT and assumes that higher temperature derivatives of the free energy are not large. For hydration free energy calculations, ΔT around 15 Kelvin is a good approximation, as indicated by agreement between calculated with the two different methods.[5,6,9,33]

Parallel Tempering. In a parallel tempering simulation, the system is replicated N times, and each replica is simulated at a different temperature. Each replica is simulated with conventional Monte Carlo (MC) or constant temperature molecular dynamics (MD), and, in addition to the local sampling of phase space, global moves are attempted which involve exchanges between replicas. The swapping moves introduce configurations from higher temperature simulations into the ensemble averages of lower temperature simulations (and vice versa). The swapping then provides a way for the lower temperature simulations to escape local minima of phase space. In the isothermal, isobaric ensemble attempted swaps of replicas i and j are accepted with a probability

$$\mathrm{acc}(i \leftrightarrow j) = \min[1, \exp(\beta_i - \beta_j)(E_i + PV_i - E_j - PV_j)] \tag{6}$$

where $\beta = 1/kT_i$, P is pressure, and V_i is the volume of replica i.[24] This method would swap both the coordinates and the

volume of the two replicas. Alternatively, the volume could not be swapped, and only the coordinates are exchanged.[24,34] In this method, the coordinates from each replica would have to be rescaled to be contained within the volume of the other replica. The acceptance probability would require a recalculation of the energy of each configuration after volume rescaling. One advantage of exchanging both the coordinates and the volume is that the energies E_i and E_j are already known, and no new energy calculations are required for the replica exchange moves. This is the method used in this study. Each replica is simulated using constant temperature, constant pressure molecular dynamics. Exchanges between neighboring replicas are attempted every 0.1 ps. After each successful exchange of coordinates at a temperature T_i to a temperature of T_j, the velocities need to be rescaled by a factor $(T_j/T_i)^{1/2}$.[34] Although not done here, replica exchange moves can also be made between replicas with different Hamiltonians, as for instance in refs 18 and 19, and in other applications.[35,36] In these cases, the acceptance probabilities are slightly different than eq 6, with terms involving the energy function of one replica with the coordinates of the other replica and vice versa.

The Weighted Histogram Analysis Method. The configurational partition function for a system at a temperature T_k is

$$Z_k(N, T, P) = e^{-\beta_k G_k} = \int \mathrm{d}\boldsymbol{r}\, \mathrm{d}V e^{-\beta_k H(\boldsymbol{r},V)} = \sum_H e^{-\beta_k H} \int \mathrm{d}\boldsymbol{r}\, \mathrm{d}V \delta(H(\boldsymbol{r}, V) - H) = \sum_H e^{-\beta_k H} \Omega_k(H) \quad (7)$$

where G_k is the Gibbs free energy, $\boldsymbol{r}$ are the system coordinates, and H is the enthalpy ($E(\boldsymbol{r})$+PV). The function $\Omega_K(H)$ is the temperature independent enthalpy density of states and can be found from a single simulation at a temperature T_k by

$$\Omega_k(H) = \int \mathrm{d}\boldsymbol{r}\, \mathrm{d}V \delta(H(\boldsymbol{r}, V) - H) = \frac{\int \mathrm{d}\boldsymbol{r}\, \mathrm{d}V e^{-\beta_k H(\boldsymbol{r},V)} \delta(H(\boldsymbol{r}, V) - H) e^{\beta_k H(\boldsymbol{r},V)}}{(Z_k/Z_k)} = \frac{e^{\beta_k H}}{1/Z_k} \frac{\int \mathrm{d}\boldsymbol{r}\, \mathrm{d}V e^{-\beta_k H(\boldsymbol{r},V)} \delta(H(\boldsymbol{r}, V) - H)}{Z_k} = e^{\beta_k H} Z_k \langle \delta(H(\boldsymbol{r}, V) - H) \rangle_k = e^{\beta_k H} e^{-\beta_k G_k} N_k(H) \quad (8)$$

where $N_k(H)$ is the histogram of enthalpies from the simulation at T_k.

The density of states can be constructed from M different simulations at M different temperatures using a weighted sum

$$\Omega(H) = \sum_{k=1}^{M} w_k(H) \Omega_k(H) = \sum_{k=1}^{M} w_k(H) N_k(H) e^{\beta_k H} e^{-\beta_k G_k} \quad (9)$$

The Ferrenberg and Swendsen optimized weights are given by[15]

$$w_k(H) = e^{-\beta_k H} e^{\beta_k G_k} / \sum_{j=1}^{M} e^{-\beta_j H} e^{\beta_j G_j} \quad (10)$$

and eq 9 becomes

$$\Omega(H) = \sum_{k=1}^{M} N_k(H) / \sum_{k=1}^{M} e^{-\beta_k H} e^{\beta_k G_k} \quad (11)$$

The Gibbs free energy at T_k can be found from

$$e^{-\beta_k G_k} = Z_k = \sum e^{-\beta_k H} \Omega(H) = \sum_H e^{-\beta_k H} \left(\sum_{j=1}^{M} N_j(H) / \sum_{j=1}^{M} e^{-\beta_j H} e^{-\beta_j G_j} \right) \quad (12)$$

Equation 12 can be solved iteratively to find the set of G_j's, provided the histogram $N_k(H)$ has some region of overlap with $N_{k+1}(H)$.

Average quantities of a property A, given by

$$\langle A \rangle_k = \int \mathrm{d}\boldsymbol{r}\, \mathrm{d}V A(\boldsymbol{r}, V) e^{-\beta_k H} / Z_k \quad (13)$$

can be expressed as

$$\langle A \rangle_k = \sum_H e^{-\beta_k H} A_k(H) / \sum_H e^{-\beta_k H} \Omega_k(H) \quad (14)$$

The function $A_k(H)$ can be found from simulation data using

$$A_k(H) \equiv \int \mathrm{d}\boldsymbol{r}\, \mathrm{d}V A(\boldsymbol{r}, V) \delta(H(\boldsymbol{r}, V) - H) = e^{\beta_k H} Z_k \int \mathrm{d}\boldsymbol{r}\, \mathrm{d}V A(\boldsymbol{r}, A) e^{-\beta_k H} \delta(H(\boldsymbol{r}, V) - H) / Z_k = e^{\beta_k H} e^{-\beta_k G_k} \langle A(H) \rangle_k \quad (15)$$

where $\langle A(H) \rangle_k$ is the average value of A for a particular value of H. Data from simulations at different temperatures can be combined using

$$A(H) = \sum_{j=1}^{M} w_j(H) A_j(H) = \sum_{j=1}^{M} w_j(H) \langle A(H) \rangle_j e^{\beta_j H} e^{-\beta_j G_j} \quad (16)$$

Putting this expression for $A(H)$ and the weights from eq 10 into eq 14 gives

$$\langle A \rangle_k = \left[\sum_H \left(\sum_j \langle A(H) \rangle_j \right) e^{-\beta_k H} / \sum_j e^{-\beta_j H} e^{\beta_j G_j} \right] / Z_k \quad (17)$$

where Z_k can be found from eq 12. Equation 17, after eq 12, is used to find the G_j's and provides a method to use data from other temperatures to calculate averages at a given temperature.

For thermodynamic integration, averages of $\langle \partial E_\lambda / \partial \lambda \rangle_\lambda$ are needed. To calculate this using eq 17 requires calculating the function $\langle \partial E_\lambda / \partial \lambda(H) \rangle_\lambda$. For free energy perturbation, the function $\langle \exp[-\beta(E_{\lambda+\Delta\lambda} - E_\lambda)](H) \rangle_\lambda$ would be needed. Other useful averages can be calculated from

$$\langle H \rangle_k = \left[\sum_H \left(\sum_j N_j(H) \right) e^{-\beta_k H} / \sum_j e^{-\beta_j H} e^{\beta_j G_j} \right] / Z_k \quad (18)$$

and

$$\left\langle H \frac{\partial E_\lambda}{\partial \lambda} \right\rangle_k = \left[\sum_H \left[H \sum_j \left\langle \frac{\partial E_\lambda}{\partial \lambda}(H) \right\rangle_j \right] e^{-\beta_k H} / \sum_j e^{-\beta_j H} e^{\beta_j G_j} \right] / Z_k \quad (19)$$

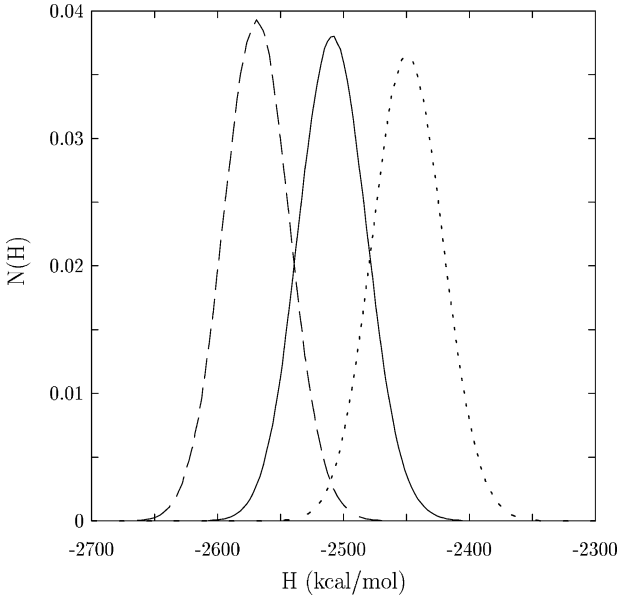

Figure 1. Histograms of the enthalpy at 283 K (dashed line), 298 K (solid line), and 313 K (dotted line), for butane in water at $\lambda = 1$.

All the averages needed to calculate ΔS from eq 3 can be found from the two functions $N_j(H)$ and $\langle \partial E_\lambda / \partial \lambda(H) \rangle_j$.

Histogram reweighting can be used to combine data not only at different temperatures but also for different Hamiltonians.[15,16] The Hamiltonian corresponding to eq 4 is not linear in λ, due to the separated-shifted scaling terms, so WHAM cannot be used to combine data at different values of λ. If the Hamiltonian were linear or another power of λ, then WHAM could be used.

Simulation Details. The simulations used 256 water molecules, treated using the TIP4P model,[37] and one solute molecule, methane or butane. The united atom, one-site OPLS model is used for methane,[38] and the all atom, OPLS-AA model is used for butane.[39] The Lorentz−Berthelot combining rules were used for the Lennard-Jones interactions, and all bonds were treated as rigid, using SHAKE.[40] The bond angles and torsional angles in butane are treated as flexible. The simulations were done in the isothermal−isobaric (constant T,P,N) ensemble, by coupling to a pressure bath (at 1 atm) and a Nosé-Hoover temperature bath for three temperatures (283, 298, and 313 K).[41−45] For this system size, the distributions of enthalpies at the neighboring temperatures have enough overlap of the enthalpy histograms for histogram reweighting and are close enough for good acceptance ratios for the parallel tempering moves (Figure 1). For butane at $\lambda = 1$, the acceptance ratio between the replicas at 283 and 298 K is 0.10 and between the 298 and 313 K replicas is 0.12. The acceptance ratios at other values of λ and for methane are similar. Long-ranged electrostatic interactions were treated using Ewald sums,[40] and no tail corrections[3,46] were made for the Lennard-Jones interactions, which were cut off at half the box length. The thermodynamic integration calculations used 15 different λ values (11 at equally spaced intervals of 0.10 from 0 to 1.0 plus 4 additional points at 0.025, 0.05, 0.15, and 0.25). Data for each λ value were generated from six 1 ns simulations, using a 1 fs time step.

Table 2. Solvation Free Energies and Error Estimates (in kcal/mol) for the Four Different Methods at Three Different Temperatures[a]

	283 K		298 K		313 K	
method	ΔG	$\delta\Delta G$	ΔG	$\delta\Delta G$	ΔG	$\delta\Delta G$
			Butane			
CMD	2.862	0.034(2)	3.180	0.034(6)	3.418	0.030(2)
CMD-WHAM	2.862	0.027(2)	3.175	0.024(5)	3.421	0.027(1)
PT	2.891	0.032(1)	3.196	0.024(2)	3.449	0.027(3)
PT-WHAM	2.886	0.029(1)	3.189	0.021(4)	3.459	0.025(3)
			Methane			
CMD	2.081	0.018(1)	2.265	0.022(3)	2.406	0.020(1)
CMD-WHAM	2.083	0.016(1)	2.268	0.015(2)	2.401	0.017(1)
PT	2.102	0.017(1)	2.252	0.015(2)	2.414	0.016(1)
PT-WHAM	2.102	0.016(1)	2.253	0.012(3)	2.414	0.014(1)

[a] Numbers in parentheses give error estimates for $\delta\Delta G$.

III. Results

Four methods to calculate the aqueous solvation free energies for the two molecules, butane and methane, are compared. The methods are as follows.

1. CMD: conventional molecular dynamics. Independent simulations at three temperatures, and for each value of λ, are used to calculate ΔG and ΔS using the thermodynamic integration eqs 2 and 3.

2. CMD-WHAM: conventional molecular dynamics plus histogram reweighting. From the independent simulations at different temperatures, the histograms $N_k(H)$ and $\langle \partial E_\lambda / \partial \lambda(H) \rangle_k$ are found. From these histograms and eqs 12 and 17−19, ΔG and ΔS can be calculated.

3. PT: parallel tempering. Parallel tempering is used to generate the ensemble averages at the three temperatures, for each value of λ.

4. PT-WHAM: parallel tempering plus histogram reweighting. From the parallel tempering simulations the histograms are found and used to calculate ΔG and ΔS.

The ΔG values are in fair agreement with the experimental values (1.932 kcal/mol for methane and 2.148 kcal/mol for butane)[47] and in good agreement with other calculated values for methane[3,4,9,48,49] and butane[3] (Table 2). Error estimates represent two standard deviations of the data calculated from

$$\delta x = \frac{2}{\sqrt{N-1}} \sqrt{\sum_{i=1}^{N} (x_i - \bar{x})^2 / N} \qquad (20)$$

where x_i is the value from the ith 1 ns simulation, and $\bar{x}$ is the average of all N x_i values. Estimates of the errors of the error bars can be made by splitting the data into halves and calculating the standard deviation of the δx values from each half. Equation 20 only gives valid error estimates if the data points are uncorrelated. The correlation time was found by calculating the time correlation function of $\langle \mathrm{d}E_\lambda / \mathrm{d}\lambda \rangle_\lambda$.[50] For $\langle \mathrm{d}E_\lambda / \mathrm{d}\lambda \rangle_\lambda$ we find that the correlation time is less than 5 ps, consistent with the results for similar models,[3] so each 1 ns simulation is uncorrelated with the others.

Differences in the error bars are in some cases not much bigger than the errors estimates in the error bars, but by looking at all six calculated free energies (3 temperatures

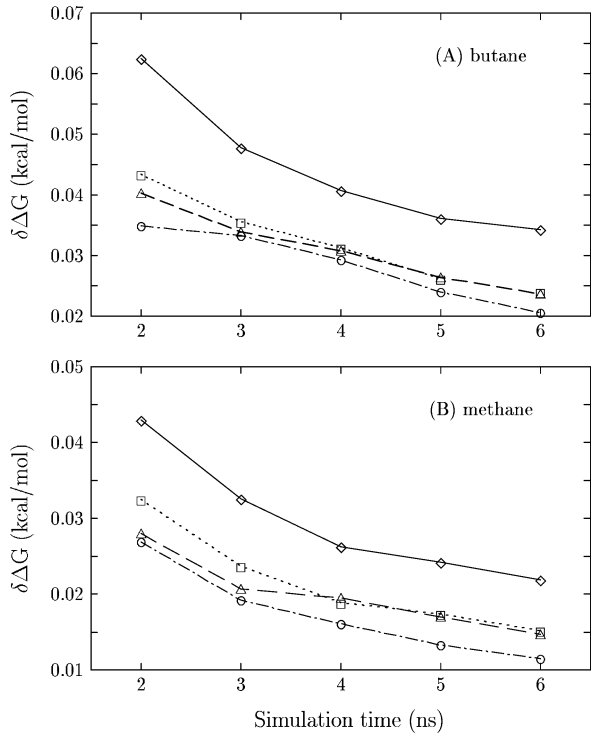

Figure 2. Error estimates of ΔG for (A) butane and (B) methane, comparing the various methods: CMD (solid line, ◇), CMD-WHAM (dotted line, □), PT (dashed line, △), and PT-WHAM (dot−dashed line, ○).

and 2 solute molecules) better assessments about the effectiveness of the different models can be made. (The error bars of the error bars are themselves difficult to determine with much precision, but they are about 5−15% of the magnitude of the $\delta\Delta G$ values, see Table 2.) When either CMD and CMD-WHAM or PT and PT-WHAM are compared, using WHAM lowers the error bars. The PT results are lower than the CMD results for all six ΔG calculations, although the CMD-WHAM results are comparable and in some cases lower than the PT or PT-WHAM results. The improvement of one method over another can be judged by looking at the ratio of the error bars. For example, for butane at 298 K, the ratio of the error bars of CMD to those of PT is (0.034 ± 0.006)/(0.024 ± 0.002) or 1.42 ± 0.27. For methane at 298, the same ratio is (0.022 ± 0.003)/(0.015 ± 0.002) or 1.47 ± 0.28. Since the error bars will decrease as the square root of the simulation time, improving the error bars by a factor of 1.4 (or $\sqrt{2}$) means error bars comparable to CMD can be achieved in half the simulation time. Figure 2 shows the error estimates for the four methods as a function of simulation length, for butane and methane at 298 K. This shows again the improvement of the PT and WHAM methods over CMD. The PT and WHAM methods give errors bars after 3 ns which are lower than CMD gives after 6 ns of simulation time. It should be kept in mind for these comparisons, that the PT and WHAM results, involving three separate simulations, use three times the computer time. As long as only ΔG values are desired, gains of $\sqrt{2}$ are not enough to overcome the need for the additional simulations. If ΔS is also desired, then simulations at other temperatures would be typically performed anyway and are not additional.

Table 3. Solvation Entropy Changes, $-T\Delta S$ (in kcal/mol) for the Four Different Methods at $T = 298$ K, Using the Two Different Entropy Expressions, Eqs 3 and 5[a]

	eq 3		eq 5	
method	$-T\Delta S$	$T\delta\Delta S$	$-T\Delta S$	$T\delta\Delta S$
		Butane		
CMD	6.14	0.69(7)	5.52	0.45(3)
CMD-WHAM	5.94	0.51(4)	5.56	0.38(2)
PT	6.45	0.75(9)	5.55	0.41(3)
PT-WHAM	5.75	0.53(3)	5.69	0.38(3)
		Methane		
CMD	2.83	0.55(8)	3.24	0.27(1)
CMD-WHAM	3.25	0.33(3)	3.17	0.23(1)
PT	3.33	0.47(7)	3.10	0.23(1)
PT-WHAM	3.13	0.42(3)	3.10	0.21(1)

[a] Numbers in parentheses give error estimates of $T\delta S$.

The entropy changes, as found from both eqs 3 and 5, are given in Table 3. The values are not too far off from the experimental values ($-T\Delta S$ is 4.8 kcal/mol for methane and 7.7 kcal/mol for butane).[47] Entropy changes have been calculated for the solvation of methane,[4,9,49] and they are close to the present values, especially for the study that used the same potential.[9] The improvement in the error bars using WHAM is about the same or slightly better for the entropy calculations, through eq 3, than it is for ΔG. Using PT does not appear to improve the error bars in the entropy calculations. The ratio of the CMD error bars over the CMD-WHAM error bars are 1.4 for butane and 1.7 for methane. This may reflect the fact that the integrand of eq 3 requires more sampling than that of eq 2. The error bars decrease more using WHAM for ΔS calculated through eq 3 than for eq 5, but still the error bars are less using eq 5. The finite difference expression, eq 5, has been previously shown to have smaller error bars.[26] The agreement in ΔS using the two different equations is very good, particularly when WHAM is used.

Histogram reweighting improves the error bars by supplementing the data at one temperature with data at other temperatures, as given by eq 17. The CMD-WHAM averages at a temperature T_k can be found from $\langle \partial E/\partial\lambda \rangle = \sum_H \langle \partial E/\partial\lambda(H) \rangle_{k,\mathrm{WHAM}}$. The function $\langle \partial E/\partial\lambda(H) \rangle_{k,\mathrm{WHAM}}$ is the sum of the appropriately weighted histograms from the CMD at three different temperatures

$$\left\langle \frac{\partial E}{\partial \lambda}(H) \right\rangle_{k,\mathrm{WHAM}} = \sum_{j=1}^{M} \left\langle \frac{\partial E}{\partial \lambda}(H) \right\rangle_j e^{-\beta_k H} / \sum_{l=1}^{M} e^{-\beta_l H} e^{\beta_l G_l} / Z_k \quad (21)$$

In Figure 3, the reweighted histograms at each of the three temperatures is shown as well as $\langle \partial E/\partial\lambda(H) \rangle_{k,\mathrm{WHAM}}$ for butane at 298 K and $\lambda = 1$. It is clear that data from all three temperatures contribute to the average. The areas under each curves are 0.925 kcal/mol (283 K), 3.46 kcal/mol (298 K), and 1.06 kcal/mol (313 K), giving a total of 5.45 kcal/mol. So 0.64 comes from the CMD simulation at 298 K (3.46/5.45), and the rest, about 1/3, comes from CMD simulations at different temperatures. The infusion of data from other temperatures helps reduce the error bars. If all WHAM did was add 1/3 more information, then using WHAM would

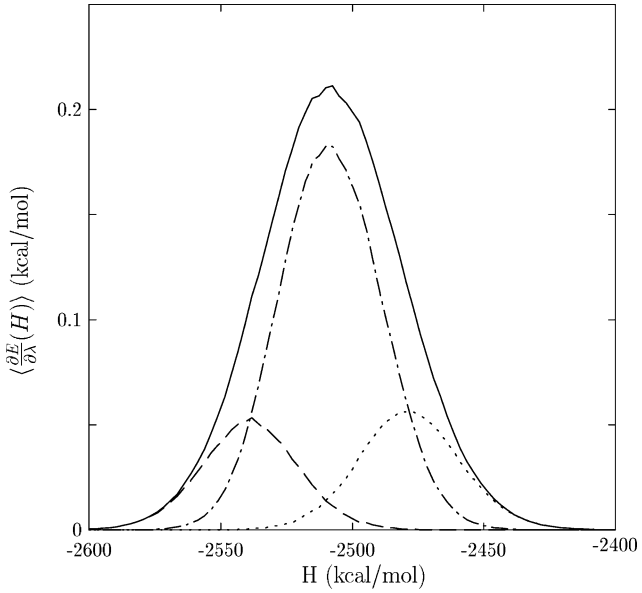

Figure 3. The function $\langle \partial E/\partial \lambda(H) \rangle$ from histogram reweighting (solid line) for butane at 298 K and $\lambda = 1$. Also shown are the reweighted histograms from CMD at 283 K (dashed line), 298 K (dot−dashed line), and 313 K (dotted line). The three reweighted histograms sum to give the solid line.

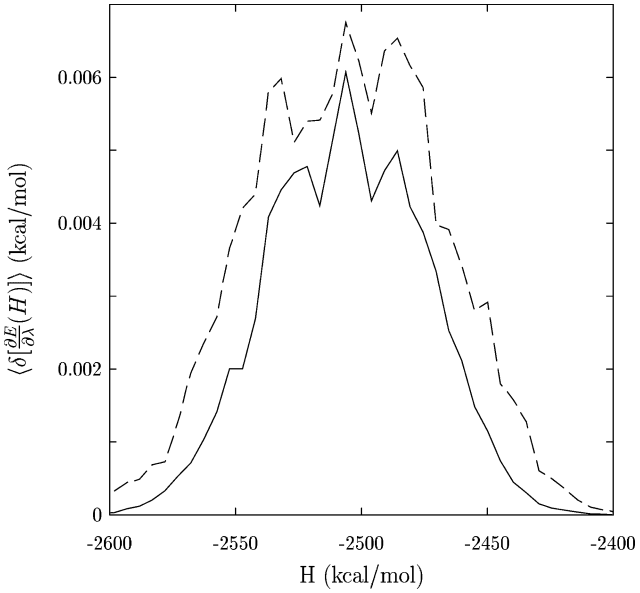

Figure 4. Error estimates of the $\langle \partial E/\partial \lambda(H) \rangle$ from histogram reweighting (solid line) and from conventional molecular dynamics (dashed line), for butane at 298 K and $\lambda = 1$.

be like running CMD for 1/3 longer, and the error bars would only be smaller by a factor of $\sqrt{4/3}$ or 1.15 instead of $\sqrt{2}$. Additional improvements in precision are found because the histograms at other temperatures preferentially sample different regions of enthalpy than the 298 K simulation and therefore increase the precision of $\langle \partial E/\partial \lambda(H) \rangle_{k,\mathrm{WHAM}}$ away from the peak. The error estimates of the histograms from CMD and from CMD-WHAM for butane at 298 K and $\lambda = 1$ shows that the errors are only slightly smaller for CMD-WHAM at the peak (around −2500 kcal/mol), because at the peak the CMD-WHAM histogram is primarily made up of the CMD histogram at 298 K. Away from the peak, the error bars are significantly smaller due the contributions from the other temperatures. Note that the largest decrease in error bars with WHAM is for the 298 K data. For the other two temperatures the decrease is not as great because data at neighboring temperatures contributes the most to the reweighted histograms and these temperatures only have one neighboring temperature, whereas 298 K combines data from two nearby temperatures.

Parallel tempering improves the error bars of the calculations but not as significantly as other applications, in which PT improves sampling efficiency by an order of magnitude.[20,51] In the study of Woods, Essex, and King which used combined PT and TI to calculate the free energy of converting a water to a methane molecule, PT (using 16 replicas, a larger number was needed in this study because it had about 6 times more molecules) reduced the error by a factor of 1.4, similar to what is found here.[18] The sampling of the aqueous methane and butane systems does not appear to involve motion over large energy barriers. If it did, then parallel tempering would improve the error bars more significantly. Also, the improvement in using PT rather than CMD would be better at low temperatures, which does not appear to be the case in this study (see Table 2). The largest

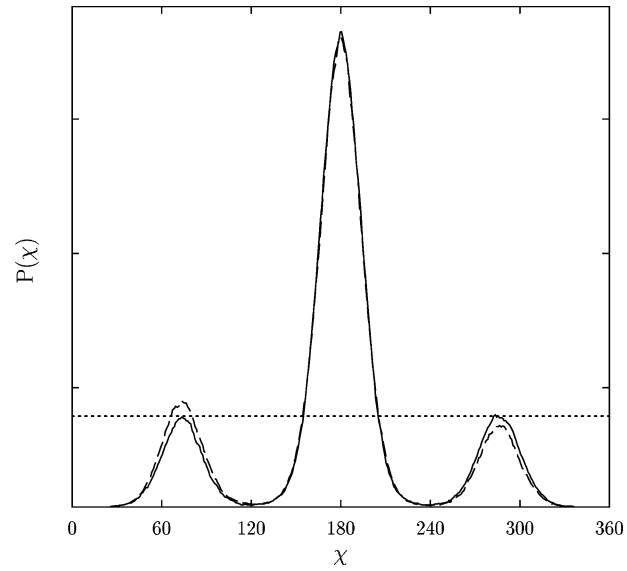

Figure 5. Distribution of the dihedral angle, χ, for butane at 283 K from 5 ns of simulations using parallel tempering (solid line) and conventional molecular dynamics (dashed line). The dotted line shows the value of the gauche peak from parallel tempering.

molecular barrier of these systems is the torsional angle of butane, involving the four carbon atoms, which a previous study has indicated may not be properly sampled over nanosecond simulations.[3] The barrier for rotation in the OPLS-AA model is 3.68 kcal/mol.[39] In our simulations, even at the lowest temperature, the torsion angle, χ, is sampled fairly adequately (Figure 5). If the sampling were completely converged, the heights of both gauche peaks (around 70 and 390 degrees) would be the same, as they are for the PT simulations, but not quite for the CMD simulations at 283 K. At 298 K and 313 K, the distribution of χ appear to be completely converged. Even though there are differences between the distributions of χ at 283 K between CMD and

PT, they are not enough to indicate large sampling problems. In addition, Shirts et al. showed that the value of ΔG was not sensitive to the value of χ.[3] These results all indicate that large barriers are not present in either of these free energy calculations. The improvements in sampling efficiency using PT is most likely not as much due to help in crossing over barriers as in providing independent trajectories.

Conclusion

The results show that notable improvements in the efficiency of calculating solvation free energies and entropies can be achieved for solvation free energies when using parallel tempering (PT) or the weighted histogram analysis method (WHAM). Error estimates when using PT and/or WHAM can be a factor or $\sqrt{2}$ less than those using conventional molecular dynamics (CMD), which means similar error bars can be achieved with simulation times half as long. The PT/WHAM error bars are lower than those of the extremely precise values of Shirts et al. which reports a ΔG of OPLS-AA butane of 3.10 ± 0.06 kcal/mol at 298 K (with 2σ error bars).[3] The calculations did not reveal that solvating a methane or a butane molecule involved sampling over large barriers. For other systems which do involve crossing barriers, use of PT would result in larger increases in the efficiency of the ΔG calculations. The WHAM method uses data generated either from CMD or PT at other temperatures to generate the quantities ($\langle \partial E_\lambda/\partial\lambda \rangle_\lambda$, $\langle H \rangle_\lambda$, and $\langle H \partial E_\lambda/\partial\lambda \rangle_\lambda$) needed to calculate ΔG and ΔS. For the temperatures and system sizes used here, there is enough overlap of the enthalpy histograms (Figure 1) to give good improvement in the precision of the free energy calculations. Both PT and WHAM are computationally inexpensive, and if simulations at additional temperatures were required to find entropy and enthalpy changes,[4−10] then using PT or WHAM does not add additional simulation time. The WHAM method is particularly easy to implement, simply requiring the calculation of two one-dimensional histograms, and can be easily combined with standard simulation programs.

Acknowledgment. This material is based upon work supported by the American Chemical Society Petroleum Research Fund under grant number 40212-GB6. A donation of hurricane relief computer time from Dr. Rigoberto Hernandez (through the National Science Foundation CRIF grant CHE 04-43564) is gratefully acknowledged.

References

(1) Beveridge, D. L.; DiCapua, F. M. *Annu. Rev. Biophys. Biophys. Chem.* **1989**, *18*, 431.

(2) Kollman, P. A. *Chem. Rev.* **1993**, *93*, 2395.

(3) Shirts, M. R.; Pitera, J. W.; Swope, W. C.; Pande, V. S. *J. Chem. Phys.* **2003**, *119*, 5740.

(4) Guilot, B.; Guissani, Y.; Bratos, S. *J. Chem. Phys.* **1991**, *95*, 3643.

(5) Smith, D. E.; Haymet, A. D. J. *J. Chem. Phys.* **1993**, *98*, 6445.

(6) Rick, S. W. *J. Phys. Chem. B* **2000**, *104*, 6884.

(7) Lüdemann, S.; Schreiber, H.; Abseher, R.; Steinhauser, O. *J. Chem. Phys.* **1996**, *104*, 286.

(8) Shimizu, S.; Chan, H. S. *J. Chem. Phys.* **2000**, *113*, 4683.

(9) Rick, S. W. *J. Phys. Chem. B* **2003**, *107*, 9853.

(10) Olano, L. R.; Rick, S. W. *J. Am. Chem. Soc.* **2004**, *126*, 7991.

(11) Geyer, C. J. In *Computing Science and Statistics: Proceedings of the 23rd Symposium on the Interface*; Interface Foundation: Fairfax Station, 1991; p 156.

(12) Marinari, E.; Parisi, G. *Europhys. Lett.* **1992**, *19*, 451.

(13) Hukushima, K.; Nemoto, K. *J. Phys. Soc. Jpn.* **1996**, *65*, 1604.

(14) Sugita, Y.; Okamoto, Y. *Chem. Phys. Lett.* **1999**, *314*, 141.

(15) Ferrenberg, A. M.; Swendsen, R. H. *Phys. Rev. Lett.* **1989**, *63*, 1195.

(16) Kumar, S.; Bouzida, D.; Swendsen, R. H.; Kollman, P. A.; Rosenberg, J. M. *J. Comput. Chem.* **1992**, *13*, 1011.

(17) Nina, M.; Beglov, D.; Roux, B. *J. Phys. Chem. B* **1997**, *101*, 5239.

(18) Woods, C. J.; Essex, J. W.; King, M. A. *J. Phys. Chem. B* **2003**, *107*, 13703.

(19) Sugita, Y.; Kitao, A.; Okamoto, Y. *J. Chem. Phys.* **2000**, *113*, 6042.

(20) Yamamoto, R.; Kob, W. *Phys. Rev. E* **2000**, *61*, 5473.

(21) Hernádez-Cobos, J.; Mackie, A. D.; Vega, L. F. *J. Chem. Phys.* **2001**, *114*, 7527.

(22) Chang, J.; Sandler, S. I. *J. Chem. Phys.* **2003**, *118*, 8390.

(23) Mitsutake, A.; Okamoto, Y. *J. Chem. Phys.* **2004**, *121*, 2491.

(24) Doxastakis, M.; Mavrantzas, V. G.; Theodorou, D. N. *J. Chem. Phys.* **2001**, *115*, 11352.

(25) Lyubatsev, A. P.; Martinsinovski, A. A.; Shevkunov, S. V.; Vorontsov-Velyaminov, P. N. *J. Chem. Phys.* **1992**, *96*, 1776.

(26) Smith, D. E.; Zhang, L.; Haymet, A. D. J. *J. Am. Chem. Soc.* **1992**, *114*, 5875.

(27) Guillot, B. *J. Chem. Phys.* **1991**, *95*, 1543.

(28) Yu, H.; Karplus, M. *J. Chem. Phys.* **1988**, *89*, 2366.

(29) Mezei, M.; Beveridge, D. L. *Ann. N. Y. Acad. Aci.* **1986**, *482*, 1.

(30) Chialvo, A. A. *J. Chem. Phys.* **1990**, *92*, 673.

(31) Zacharias, M.; Straatsma, T. P.; McCammon, J. A. *J. Chem. Phys.* **1994**, *100*, 9025.

(32) Rick, S. W.; Berne, B. J. *J. Am. Chem. Soc.* **1996**, *118*, 672.

(33) Lüdemann, S.; Abseher, R.; Schreiber, H.; Steinhauser, O. *J. Am. Chem. Soc.* **1997**, *119*, 4206.

(34) Bedrov, D.; Smith, G. D. *J. Chem. Phys.* **2001**, *115*, 1121.

(35) Fukunishi, H.; Watanabe, O.; Takada, S. *J. Chem. Phys.* **2002**, *116*, 9058.

(36) Jang, S.; Shin, S.; Pak, Y. *Phys. Rev. Lett.* **2003**, *91*, 058305.

(37) Jorgensen, W. L.; Chandrasekhar, J.; Madura, J. D.; Impey, R. W.; Klein, M. L. *J. Chem. Phys.* **1983**, *79*, 926.

(38) Jorgensen, W. L.; Madura, J. D.; Swenson, C. J. *J. Am. Chem. Soc.* **1984**, *106*, 6638.

(39) Jorgensen, W. L.; Maxwell, D. S.; Tirado-Rives, J. *J. Am. Chem. Soc.* **1996**, *118*, 11225.

(40) Allen, L. C. *Acc. Chem. Res.* **1990**, *23*, 175.

(41) Andersen, H. C. *J. Chem. Phys.* **1980**, *72*, 2384.

(42) Ciccotti, G.; Ryckaert, J. P. *Comput. Phys. Rep.* **1986**, *4*, 345.

(43) Martyna, G. J.; Tobias, D. J.; Klein, M. L. *J. Chem. Phys.* **1994**, *101*, 4177.

(44) Nosé, S. *Mol. Phys.* **1984**, *52*, 255.

(45) Hoover, W. G. *Phys. Rev. A* **1985**, *31*, 1695.

(46) Frenkel, D.; Smit, B. *Understanding Molecular Simulation: from Algorithms to Applications*; Academic Press: San Diego, CA, 1996.

(47) Ben-Naim, A.; Marcus, Y. *J. Chem. Phys.* **1984**, *81*, 2016.

(48) Jorgensen, W. L.; Blake, J. F.; Buckner, J. K. *Chem. Phys.* **1989**, *129*, 193.

(49) Guillot, B.; Guissani, Y. *J. Chem. Phys.* **1993**, *99*, 8075.

(50) Swope, W. C.; Andersen, H. C.; Berens, P. H.; Wilson, K. R. *J. Chem. Phys.* **1982**, *76*, 637.

(51) Yan, Q.; de Pablo, J. J. *J. Chem. Phys.* **2000**, *113*, 1276.

CT050207O